Effect of quasi-two-dimensional Fermi surfaces on electronic properties in $YbSb_2$

N. Sato, T. Kinokiri, and T. Komatsubara
Physics Department, Graduate School of Science, Tohoku University, Sendai 980-8578, Japan

H. Harima
The Institute of Scientific and Industrial Research, Osaka University, Ibaraki, Osaka 567-0047, Japan
(Received 1 October 1998)

We have measured the electrical resistivity $\rho(T)$, magnetization $M(H)$, and the de Haas–van Alphen (dHvA) effect of $YbSb_2$ which is a type-I superconductor having a layerd crystal structure. We have also performed a band structure calculation, and its comparison with observed dHvA signals indicates that there exists a quasi-two-dimensional Fermi surface (FS), reflecting the anisotropic crystal structure. The dHvA effect was also detectable by a commercial SQUID magnetometer, which directly measures $M(H)$ and allows us to determine its absolute value. We have observed an excellent agreement in an amplitude of $M(H)$ with a formula derived from the so-called Lifshitz-Kosevich theory, but a departure in a phase from it. The latter may be ascribed to the two-dimensional nature of the FS. A T^2 law of $\rho(T)$ observed at low temperatures has been attributed to phonon scatterings of carriers having the cylindrical FS with a small diameter.
[S0163-1829(99)03807-2]

I. INTRODUCTION

Rare-earth diantimonides RSb_2 (R=rare-earth element) crystallize in the orthorhombic $SmSb_2$ type crystal structure for a light rare-earth element and in the orthorhombic $ZrSi_2$ type for a heavy rare-earth element.[1] Light rare-earth diantimonides show a variety of physical properties including superconductivity, antiferromagnetism, and metamagnetism.[2] Ytterbium diantimonide $YbSb_2$ is also of $ZrSi_2$ type, in which two kinds of sheets consisting only of Sb atoms and of both Yb and Sb atoms are stacked along the b axis.[3] The lattice constant of the b axis exceeds 16 Å, which is four times as large as that of the a and c axis. The layered crystal structure may remind us of that of high T_c cuprates. So far it has been claimed that $YbSb_2$ is a type-I superconductor with a superconducting transition temperature $T_c \sim 1$ K.[4] However, detailed investigations on $YbSb_2$ have been rarely reported and its electronic states remain unclear,[5] probably because it is difficult to grow a crystal which contains no other phases such as Sb, YbSb, and oxides. Thus one of the purposes of the present study is to prepare a single crystal of good quality, which is sufficient to observe the de Haas–van Alphen (dHvA) effect, to reveal intrinsic electronic properties of $YbSb_2$.

Quantum oscillations in a strong magnetic field appear in many physical quantities, such as magnetization $M(H)$, electrical resistivity $\rho(T)$, specific heat $C(T)$, etc.[6] From an analysis of these oscillatory behaviors we can obtain direct informations about the anisotropy of the Fermi surface (FS). For detection of oscillations of $M(H)$, i.e., the dHvA effect, there are several well-known methods. The field modulation (FM) method has been most thoroughly developed, in which a sample is put into one of a balanced pair of pick-up coils, and $M(H)$ is made to vary periodically with time by superimposing a small periodic field $h_0 \cos \omega t$, and then an induced electromotive force (emf) at the same frequency ω (or at a higher frequency) is examined. A pulsed field technique is another dynamical method. If the field is varied with time, a sample placed in pick-up coils gives the emf voltage proportional to dM/dt. This method needs no periodic modulation fields, but it may require a rapid variation of the pulsed field, and thus it seems to be inadequate for low temperature experiments. However, this difficulty was overcome by Sato *et al.* by utilizing a high sensitivity of a superconducting quantum interference device (SQUID).[7] These dynamical methods detect a voltage proportional to dM/dH, whereas a static method measures the magnetization $M(H)$ directly. Recent progress in a (commercial) SQUID magnetometer, which should be distinguished from the above mentioned technique using SQUID, enables us to easily detect the dHvA oscillation. In this method a voltage in a coil system induced by moving a sample with respect to the fixed coil system is in proportion to $M(H)$ and is picked up by the SQUID. The static method is of great advantage to determination of the absolute value of $M(H)$, which may give more detailed information about FS in comparison with the dynamical methods, as will be explained in a following section.

In the present paper, we will present the experimental and calculated results of FS, which show the existence of a quasi-two-dimensional (2D) FS of $YbSb_2$. We will suggest the effect of such a FS on the dHvA oscillatory behavior. Furthermore scattering mechanisms of $\rho(T)$ will be discussed on the basis of the obtained FS.

II. EXPERIMENTAL AND CALCULATION METHODS

Single crystals were prepared using a usual Bridgman method. The appropriate amount of constituents, 99.9% (3N) pure Yb and 5N Sb, were melted in ''double-sealed'' quartz tubes at about 900 °C, and then they were cooled down slowly, typically at a speed of a few Kelvins per hour. An obtained ingot was about 12 and 20 mm in diameter and in length, respectively, and it was found to consist of several single crystals, the typical dimensions being several millime-

ters along the *a* and *c* axis and 0.5–3 mm along the *b* axis. It was easily cleaved at the *b* plane (*a*-*c* plane) reflecting the layered crystal structure. A powder x-ray-diffraction method confirmed the $ZrSi_2$-type crystal structure, and a electron probe microanalyzer indicated a single phase of $YbSb_2$, although we found a few ingots to contain thin layers of Sb phase which were sandwiched between the $YbSb_2$ phases. The single crystals were cut by a spark erosion cutter for $\rho(T)$ and $M(H)$ measurements. The electrical resistivity was measured by a conventional four probe method, and the magnetization measurements were made by a commercial SQUID magnetometer in external magnetic fields up to 5 T in a ^{4}He cryostat and by the FM technique ($\omega \sim 1.3$ kHz) in a ^{3}He cryostat with an 8 T superconducting magnet.

Band structure calculations are carried out using a full-potential linear augmented-plane-wave (FLAPW) method with the local density approximation (LDA) for the exchange correlation potential. However, we adopted a constant potential for Yb-4*f* electrons to obtain proper Fermi surfaces as will be mentioned later. For the LDA, the formula proposed by Gunnarsson and Lundqvist[8] is used. For the band structure calculation, we used the program codes; TSPACE (Ref. 9) and KANSAI-94. The scalar relativistic effects are included for all electrons and the spin-orbit interactions are included for valence electrons as a second variational procedure. MT radii are set as $0.3575a$ for Yb and as $0.3093a$ for both Sb, where *a* is a lattice constant of the *a* axis. Core electrons (Xe core except $5p^6$ for Yb and Kr core for Sb) are calculated inside the MT spheres in each self-consistent step. $5p^6$ electrons on Yb and $4d^{10}$ electrons on Sb are calculated as valence electrons with the second energy window.

The LAPW basis functions are truncated at ($|k+G_i| \leq 4.35(2\pi/a)$, corresponding to 575 LAPW functions at the Γ point. 70 sampling *k* points in the irreducible Brillouin zone (BZ) are used for potential convergence. To give final band structures, eigenenergies are calculated at 473 *k* points for the irreducible BZ.

For Yb compounds, Yb-4*f* bands occasionally lie very close to the Fermi level to affect Fermi surfaces due to the insufficient treatment of 4*f* electrons in the LDA. In fact, we find that the Yb-$4f_{j=7/2}$ level is situated around only 0.01 Ry below the Fermi level, while the photoemission spectrum indicates that the Yb-4*f* states lie about 0.05 Ry below E_F.[10] This implies that the Yb-4*f* states are fully occupied, and thus that the Yb ion is of the $Yb^{2+}(4f^{14})$ ground state. Then we have carried out another self-consistent calculation with the 4*f*-level artificially shifted downward by 0.2 Ry, which gives the Yb-$4f_{j=7/2}$ level 0.1 Ry below the Fermi level after the self-consistent step. In this paper, we show the result given by such a treatment.

III. RESULTS AND DISCUSSION

A. Experimental and calculated results of FS

Figure 1 shows the crystal structure of $YbSb_2$, which is of the orthorhombic $ZrSi_2$ type. The unit cell is prolonged along the *b* axis, and lattice constants are $a=4.561$ Å, $b=16.72$ Å, and $c=4.268$ Å at room temperature. In this structure two kinds of layers are stacked along the *b* axis; one consists only of Sb (I) atoms and the other of Yb and Sb (II) atoms.

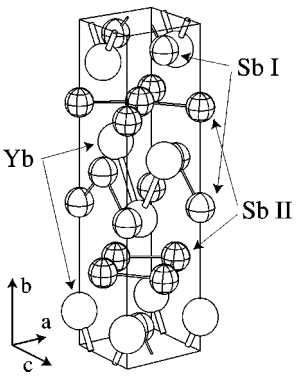

FIG. 1. Crystal structure of $YbSb_2$. Note the layered structure.

Figure 2 indicates typical dHvA oscillations, which were detected by the conventional FM method at $T=0.5$ K for external magnetic fields applied along the *b* axis. A period of oscillation in an inverse field space, *F*, corresponds to a cross section of extremal area of FS perpendicular to the field direction, *A*, which can be related to *F* through the equation $F=(c\hbar/2\pi e)A$. The fast Fourier transform (FFT) given in the inset shows that there are several extremal areas perpendicular to the *b* axis. We show the angular dependence of *F* together with the calculated one in Fig. 3, in which one may see a rather good agreement between them except a difference in the absolute value by a factor of 1–2.[11] We notice that there exist several branches which have a minimum about the *b* axis; for instance, the *a* branch (depicted in the inset to Fig. 2) shows an angular dependence which is approximated by $F_0/\cos\theta$, in which θ denotes an angle of the external field from the *b* axis and $F_0=2.36\times10^6$ Oe. This branch may correspond to the calculated one which is referred to as α having a frequency of 3.0×10^6 Oe indicated in Fig. 3. In Fig. 4 we show the calculated FS, two electron surfaces and one hole surface, and we suggest that these FS are derived mainly from Sb *p* states. The coexistence of electronlike and holelike carriers may be consistent with preliminary results of the Hall effect experiments which show a

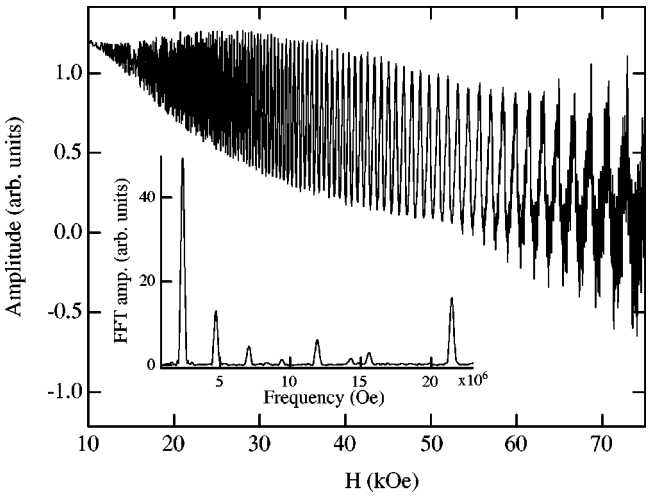

FIG. 2. Typical de Haas–van Alphen oscillations detected by a conventional field modulation method. The inset shows its fast-Fourier-transformed spectrum.

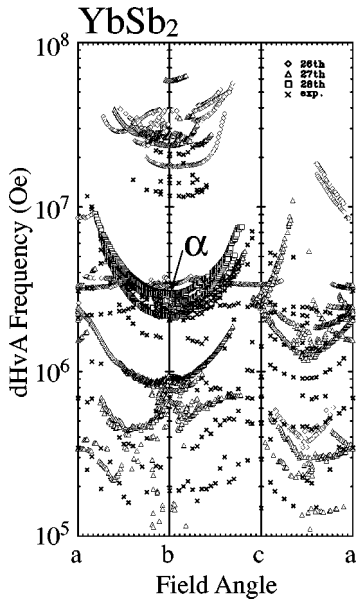

FIG. 3. Angular dependence of the measured and calculated cross sectional area.

change of the sign at a low temperature. The α-branch corresponds to an orbit circulating on the cylindrical FS illustrated in Fig. 4(c), in which one may find the two-dimensional-like feature. Very recently a similar angular dependence of the frequency was claimed as an indication of a quasi-2D FS for $SmSb_2$.[12] Thus this nature is considered to originate from the layered crystal structure, although the crystal structure of these two compounds is slightly different.

Figure 5 indicates the calculated energy bands, in which the Yb-4f bands artificially shift downward as mentioned above. This band structure suggests the nonmagnetic Yb^{2+} state, in coincidence with the experimental results of the magnetic susceptibility $\chi(T)$ which is small (-1.4×10^{-4} emu/mole) and nearly temperature independent (above about 100 K).

We determined an effective cyclotron mass m and the Dingle temperature T_D from the temperature and field-strength dependence of the dHvA signal amplitude, respectively. For the a branch, we have $m_{exp}=0.118m_0$ and $T_D=2.3$ K for $H//b$ axis, where m_0 denotes the cyclotron mass of a free electron. The corresponding calculated cyclotron mass is $m_{cal}=0.08m_0$. The effective cyclotron masses of the other observed branches are in the range of 0.1–0.4. These small effective masses may be compatible with a small electronic specific heat coefficient $\gamma_{exp}=5\pm1$ mJ/K^{2}mole (not shown here), which is twice as large as that estimated from the calculated density of states at E_F, $\gamma_{cal}=2.1$ mJ/K^{2}mole. The ratio of γ_{exp} to γ_{cal} looks to be larger than m_{exp}/m_{cal}. Since γ corresponds to an average over the whole FS, the difference in the mass enhancement between γ and m may suggest that there should be other branches having heavier cyclotron masses which could not be observed in the present experiment. It may be possible to assume that the mass enhancement of about 2 is due to a nontrivial contribution from the Yb-4f states in the electronic state at E_F.

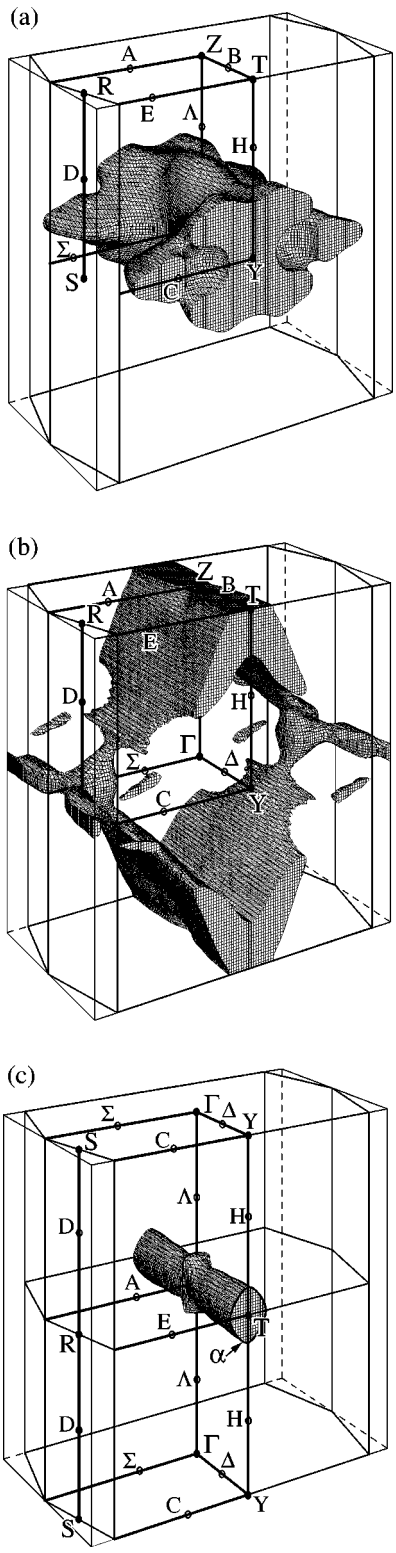

FIG. 4. Fermi surfaces of $YbSb_2$; (a) a hole surface derived from the 26th band, (b) an electron surface from the 27th band, and (c) a cylindrical electron surface from the 28th band.

B. Quantum oscillations of $M(H)$ detected by the static method

As mentioned in the Introduction, a SQUID magnetometer is able to directly measure $M(H)$. The so-called Lifshitz-Kosevich theory yields a standard formula for the oscillatory part of $M(H)$ as follows,[6]

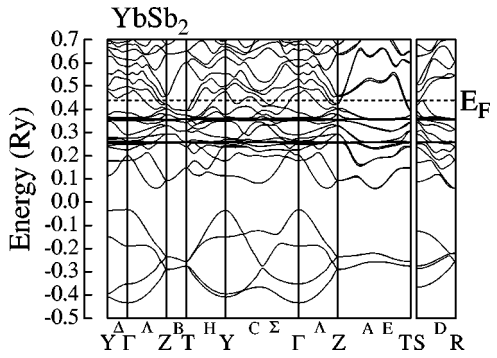

FIG. 5. Electronic band structure of $YbSb_2$, where the occupied $4f$ bands on Yb are artificially shifted downward.

$$\tilde{M} = A_{\mathrm{mp}} \sin\left(\frac{2\pi F}{H} + \phi\right), \tag{3.1a}$$

$$A_{\mathrm{mp}} = -2.6\times 10^{-2}\left(\frac{2\pi}{A''}\right)^{1/2} \frac{GFT}{\sqrt{H}} \frac{\exp(-\alpha T_D/H)}{\sinh(\alpha T/H)}, \tag{3.1b}$$

where

$$A'' = \left|\frac{\partial^2 S}{\partial \kappa^2}\right|_{\kappa=0},$$

$$G = \cos\left(\frac{\pi}{2} g \frac{m}{m_0}\right),$$

and

$$\alpha = 1.47\times 10^5 (m/m_0)$$

in CGS units. (For simplicity, we consider only the fundamental and omitted summation over different frequencies F.) Here, S denotes the cross section at an arbitrary κ which is a component of the wave number vector in the H direction, g is a spin-splitting factor, and ϕ is a phase constant. On the other hand, the e.m.f. voltage v produced by the FM technique is proportional to $\mathrm{d}\tilde{M}/\mathrm{d}H$ and is given by the following:

$$v = -2c\omega A_{\mathrm{mp}} \sum_{k=1}^{\infty} kJ_k(\lambda) \sin\left(\frac{2\pi F}{H} + \phi - \frac{k\pi}{2}\right) \sin k\omega t, \tag{3.2}$$

where c is an appropriate coupling constant, $J_k(\lambda)$ is the kth Bessel functions of $\lambda = 2\pi h_0/\Delta H$, and $\Delta H = H^2/F$ denotes the field interval of one dHvA oscillation. As may be seen from Eq. (3.2), Bessel functions make it rather complicated to determine A_{mp} experimentally, in contrast to Eq. (3.1).

We found the low-T magnetization isotherm $M(H)$ to show a rapid oscillation which is demonstrated in Fig. 6. We also illustrated the calculated curve in terms of Eq. (3.1) with a following set of parameters; $F = 2.36\times 10^6$ Oe, $m/m_0 = 0.118$, $T_D = 2.3$ K which were obtained by the FM method, as mentioned above. This excellent coincidence clearly shows that the oscillation is really the dHvA effect.[13] We determined the absolute value of $\tilde{M}$, which will lead to $|G|/\sqrt{A''} = 0.732$. Here, the sign of G depends on the choice

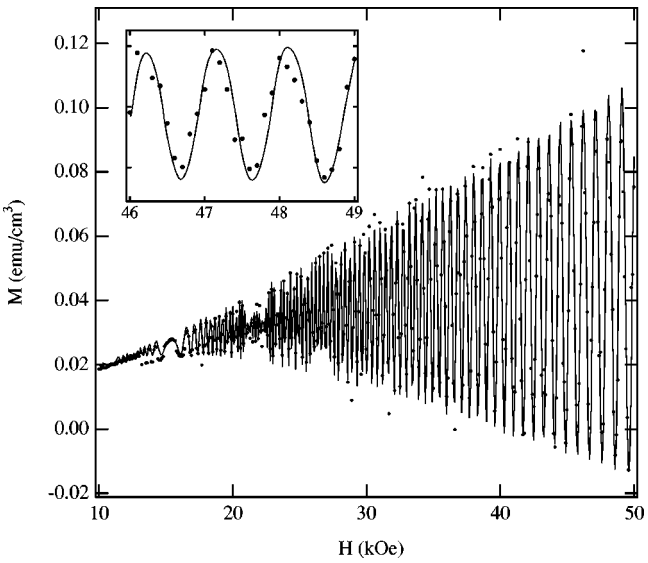

FIG. 6. Quantum oscillations of the magnetization detected by a commercial SQUID magnetometer. The solid line depicts the calculated result in terms of the so-called Lifshitz-Kosevich theory. Note the excellent agreement between them. The inset shows the results in an expanded scale, in which the phase in the calculation indicated by the solid line is shifted by $-60°$ from the conventional value $3\pi/4$.

of the phase ϕ (see below). Since FFT of the present dHvA oscillation produces only one component of frequency, the field interval between adjacent peaks should become small monotonically as the field is decreased. The discrepancy from this expected behavior which is particularly obvious at $H\sim$ 15 kOe is probably ascribed to an experimental condition that the measurements were performed at an interval of 50 Oe, which is comparable to the period of the oscillation $\Delta H \sim 100$ Oe at $H = 15$ kOe. (The calculation was also made at the same fields as the experiment, and the points were connected by the solid line.)

In this calculation we added a term $\chi_0 H (\chi_0 = +3.7\times 10^{-7}$ emu/cm^3) to include a contribution from a nonoscillatory part of $M(H)$, in addition to $B_J(H)$ which denotes the Brillouin function to take into account of a magnetic impurity contribution. If we assume a free Yb^{3+} ion as the impurity, then the concentration was estimated as 260 ppm. Here, one may notice that the above value of χ_0 is positive in contrast to the negative high-temperature susceptibility mentioned above. This implies that there may be an intrinsic weakly temperature-dependent paramagnetic component in the total magnetic susceptibility, in other words, a rise in $\chi(T)$ observed at low temperature is partially of intrinsic origin. Unfortunately, we are not able to discuss the magnetic susceptibility on the basis of the calculated band structure, because it was impossible to extract the band-electrons contribution from the measured magnetic susceptibility, which contains core-electrons contribution.

The cylindrical shape of the 28th band FS shown in Fig. 4(c) implies that k dependence in the cross section of the FS is weak along the b^* axis. The significant feature of such a surface is that the curvature factor A'' becomes vanishingly small and higher terms $A^{(n)}$ need to be considered. As the actual FS exhibits complicated structures, A'' is nonvanish-

ing, but it is still so small that the exact value of A'' is hardly obtained by the band-structure calculation, which predicts $A'' \leqslant 0.1$. For such a case modifications may be required in the standard formula, which gives $\phi = 2\pi(-\gamma_0 \pm \frac{1}{8}) = -2\pi\gamma_0 \pm \frac{1}{4}\pi$, where $\pm$ indicates whether the extremal area is minimum $(+)$ or maximum $(-)$, and γ is the Onsager phase factor, normally expected to be close to 1/2.[6] Note that the band structure calculation shows that the α-branch has a curvature corresponding to the maximum, as may be seen from Fig. 4(c), thus we would expect $\phi = (3\pi/4) + 2n\pi$, where n = integer. However, the fitting produces $\phi = 5\pi/12$. This shift in ϕ (by -60 degrees) is possibly ascribed to the quasi-2D feature of the FS. (See Appendix 5.2 in Ref. 6 for fully comprehensive discussions.)

The estimation of ϕ leads to the minus sign of G, and thus we have $G = -0.23$. Here, we assumed $A'' = 0.1$. This eventually yields $g_0 = 9.7$, where g_0 is the smallest (positive) value of g factor among a possible set of values.[6] This considerable departure from a free electron value of 2 may be due to the spin-orbit coupling and/or many-body interactions, the former being particularly important in small pieces of FS.[6]

Briefly we comment on the comparison of the results obtained by the FM and static method. As shown in Fig. 2, the FFT spectrum obtained by the FM method shows several frequency components, whereas the static method given in Fig. 6 provides only one component. Thus, the latter seems to have a poorer sensitivity. But this is not true, because the difference in those spectra is simply attributed to the difference in field windows of the FFT; the spectrum shown in Fig. 2 was obtained by FFT in the region of 60–75 kOe, and if we made Fourier transform of this signal in the same field region as the static method, i.e., $H \leqslant 50$ kOe, then we obtain a similar spectrum consisting of one component. On the other hand, the oscillation of $M(H)$ in Fig. 6 does not fall off with H in comparison with that in Fig. 2. This may imply that the static method is useful for high-field measurements, although shieldings of the SQUID from strong magnetic fields may not be easy.

C. T^2 dependence of $\rho(T)$ at low temperature

Figure 7 shows the temperature dependence of the electrical resistivity. The electrical current flowing I was directed along the principal crystallographic directions, a, b, and c axis, and $\rho(T)$ for the $I \| b$ axis, ρ_b, was largest among them. We found that the resistance ratio, $\rho(300)/\rho(4.2)$, amounts to about 120 for all directions, implying a good quality of the sample. An in-plane anisotropy (i.e., an anisotropy within the a-c plane) was small, while the anisotropy $\rho_b/\rho_{a,c}$ ranges from 8 to 10 at room temperature, which is slightly sample dependent. This large anisotropy preferring the electrical current flowing in the a-c plane probably reflects the layered crystal structure.

The inset demonstrates an onset of the superconducting transition at $T_c \sim 1$ K, which also varied from sample to sample. The magnetic susceptibility measurements enabled us to determine a superconducting critical magnetic field $H_c(T)$ (not shown here), which was found to be isotropic and follow a usual T^2 law; $H_c(T) = H_c(0)[1-(T/T_c)^2]$[$H_c(0) = 66$ Oe and $T_c = 1.37$ K]. By using these values of $H_c(0)$ and γ, we estimated an energy gap at zero temperature as $\Delta(0) = 2.2$ K, leading to $2\Delta(0)/k_B T_c = 3.5$, which is a typical BCS value.

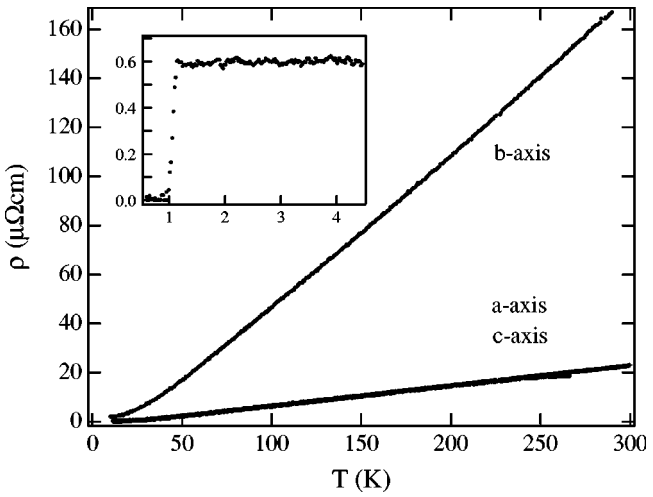

FIG. 7. Temperature dependence of the electrical resistivities. Note the large anisotropy possibly reflecting the layered crystal structure. Inset indicates an onset of superconductivity below $T_c \sim 1$ K.

We observe a T-linear dependence of $\rho(T)$ in a wide temperature range above about 50 K. There was a sample to show a break of the slope around ~ 240 K, similarly to $PrSb_2$.[2] However, since no anomaly was observed in other physical quantities even in the ''anomalous'' specimen, the origin of the anomaly remains unclear. The fitting of $\rho(T)$ at high temperatures to the so-called Bloch-Grüneisen formula produced a Debye temperature $\theta_D \sim 170$ K, which may be compatible with $\theta_D = 140$ K deduced from the coefficient of the T^3 term of the specific heat, $\beta = 0.65$ mJ/K^{4}mol. This relatively small Debye temperature is considered to be an origin of the above T-linear dependence in the wide temperature range below room temperature.

It is interesting to note a T^2 dependence of $\rho(T)$ at temperatures lower than about 45 K (see Fig. 8), and let us discuss the scattering mechanism. We obtained a coefficient of the T^2 term as $A_b = 7.5 \times 10^{-3}\mu\Omega$ cm/K^2 ($A_{a,c} = 9.2$

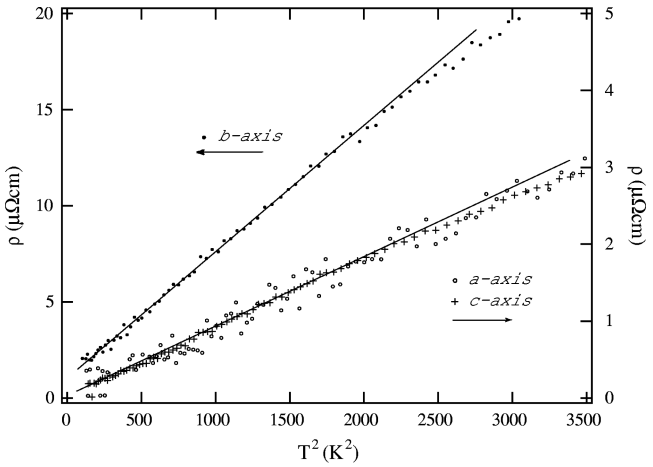

FIG. 8. T^2 dependence of the electrical resistivity, which may be ascribed to the carrier-phonon interaction. See text for details.

$\times 10^{-4}\mu\Omega$ cm/K^2) for $I\|b$ axis ($I\|a$ and c axis). At first insight, it reminds us of the carrier-carrier collision mechanism, which is often observed in heavy fermion compounds. However, this may not be the case, because the ratio of A_b to γ^2 reaches $A_b/\gamma^2 \sim 300$, which is much larger than the expected value of the order of 10 for heavy Fermi liquids and other strongly correlated metals.[14] (Even if we use $A_{a,c}$ instead of A_b, then the ratio is still as large as 37.) Alternatively, it may be possible to ascribe it to the carrier-phonon interaction. As is well known, the phonon contribution to $\rho(T)$ shows a T^5 dependence at low temperatures, and thus this possibility could be discarded. However, it should be remembered that for a small cylindrical Fermi surface there may exist an intermediate temperature interval $T_p \leqslant T \leqslant T_k$ in which the resistivity varies purely as T^2. According to a theory by Kukkonen, T_p and T_k can be determined from the size of the FS through the relations $T_p = 2\hbar s p_F/k_B$ and $T_k = 2\hbar s k_F/k_B$, respectively, where s is the sound velocity, and $2p_F$ ($2k_F$) is the diameter (height) of the cylindrical Fermi surface.[15] If we make a rough estimation for them, $s = 2\times 10^5$ cm/s, $2p_F = 1.7\times 10^7$ cm^{-1}, and $2k_F = 3.8 \times 10^7$ cm^{-1}, then we obtain $T_p = 25$ K and $T_k = 56$ K.[16] Here we modeled the FS of the 28th-band as the cylinder, which has an area $\pi p_F^2 (2\pi e/c\hbar) F_0$ and the height given by the dimension of the Brillouin zone along the b^* axis. These values of T_p and T_k seem to explain the experimental results, suggesting that the electrical currents are carried mainly by the quasi-2D FS shown in Fig. 4(c).

IV. CONCLUSIONS

We have measured the dHvA effect and constructed Fermi surfaces (FS) of $YbSb_2$ and showed the existence of the FS of a quasi-two-dimensional nature. From an experimental point of view, we stress that the dHvA effect was detectable by means of a commercial SQUID magnetometer, which allows us to determine the absolute value of $M(H)$. The direct comparison of $M(H)$ with the formula derived from the Lifshitz-Kosevich theory showed the excellent agreement in the amplitude. On the other hand, we observed the phase-shift from the expected value for a usual three-dimensional case, and we ascribed it to the quasi-2D nature of the FS. Such an anisotropy of the FS may cause the anisotropic electrical resistivity. We also estimated the spin-splitting factor $g_0 = 9.7$, which is considerably deviated from the free electron value of 2. This difference may be attributed to the spin-orbit coupling in the cylindrical FS with the small diameter. Finally we have suggested that the T^2 dependence of $\rho(T)$ at low temperatures is ascribed to the carrier-phonon scattering mechanism in the quasi-2D FS.

ACKNOWLEDGMENTS

One of the authors (N.S.) thanks Dr. T. Suzuki and Dr. T. Takahashi for kindly informing him of the experimental data before publishing.

[1] F. Hullinger, in *Handbook on the Physics and Chemistry of Rare Earths*, edited by K.A. Gschneidner, Jr. and J. Eyring (North-Holland, Amsterdam, 1979), Vol. 4.

[2] S. L. Bud'ko, P. C. Canfield, C. H. Mielke, and A. H. Lacerda, Phys. Rev. B **57**, 13 624 (1998).

[3] R. Wang, R. Bodnar, and H. Steinfink, Inorg. Chem. **5**, 1468 (1966).

[4] Y. Yamaguchi, S. Waki, and K.Mitsugi, J. Phys. Soc. Jpn. **56**, 419 (1987).

[5] R. E. Bodnar, H. Steinfink, and K. S. V. L. Narasimhan, J. Appl. Phys. **39**, 1485 (1968).

[6] D. Shoenberg, *Magnetic Oscillations in Metals* (Cambridge University Press, Cambridge, 1984).

[7] N. Sato, H. Aono, Y. Inada, A. Sawada, and T. Komatsubara, Jpn. J. Appl. Phys., Part 2 Part 2 **32**, L207 (1993).

[8] O. Gunnarsson and B.I. Lundqvist, Phys. Rev. B **13**, 4274 (1976).

[9] A. Yanase, *Fortran Program for Space Group*, 1st ed. (Shokabo, Tokyo,1995) [in Japanese].

[10] T. Takahashi (unpublished).

[11] Some branches were not detected, and, as usual, it may be ascribed to heavy cyclotron masses of those branches.

[12] C. H. Mielke, N. Harrison, A. H. Lacerda, S. H. Bud'ko, and P. C. Canfield, J. Phys.: Condens. Matter **10**, 5289 (1998).

[13] Such an observation of the oscillation by using a SQUID magnetometer was recently reported for $SmSb_2$ (see Ref. 12) and was also successfully measured for Al [T. Suzuki (unpublished)].

[14] K. Miyake, T. Matsuura, and C. M. Varma, Solid State Commun. **71**, 1149 (1989), and references therein.

[15] C. A. Kukkonen, Phys. Rev. B **18**, 1849 (1978).

[16] The sound velocity measured by T. Suzuki is temperature dependent. Therefore, the value of s used in the text should be recognized as an approximate one for estimation of T_p and T_k.